12-1-2016

# A Tale of Two Antennules: The Performance of Crab Odor-Capture Organs in Air and Water

Lindsay D. Waldrop
*Chapman University*, waldrop@chapman.edu

Laura A. Miller
*University of North Carolina at Chapel Hill*

Shilpa Khatri
*University of California, Merced*



## Recommended Citation

L.D. Waldrop, L.A. Miller, S. Khatri. 2016. A tale of two antennules: The performance of crab odor-capture organs in air and water. *Journal of the Royal Society Interface* 13: 20160615. https://doi.org/10.1098/rsif.2016.0615

# A Tale of Two Antennules: The Performance of Crab Odor-Capture Organs in Air and Water

# A tale of two antennules: The performance of crab odour-capture organs in air and water

Lindsay D. Waldrop[1], Laura A. Miller[2], and Shilpa Khatri[1]

[1]Applied Math Unit, School of Natural Sciences, University of California, Merced, CA, USA

[2]Depts. of Biology and Mathematics, University of North Carolina, Chapel Hill, NC, USA

November 16, 2016

**Abstract**

Odour capture is an important part of olfaction, where dissolved chemical cues (odours) are brought into contact with chemosensory structures. Antennule flicking by marine crabs is an example of discrete odour capture (sniffing) where an array of chemosensory hairs is waved through the water to create a flow-no flow pattern based on a narrow range of speeds, diameters of, and spacings between hairs. Changing the speed of movement and spacing of hairs at this scale to manipulate flow represents a complicated fluid dynamics problem. In this study, we use numerical simulation of the advection and diffusion of a chemical gradient to reveal how morphological differences of the hair arrays affect odour capture. Specifically, we simulate odour capture by a marine crab (*Callinectes sapidus*) and a terrestrial crab (*Coenobita rugosus*) in both air and water to compare performance. We find that the antennule morphologies of each species are adaptions to capturing odours in

their native habitats. Sniffing is an important part of odour capture for marine crabs in water where the diffusivity of odourant molecules is low and flow through the array is necessary. On the other hand, flow within the hair array diminishes odour-capture performance in air where diffusivities are high. This study highlights some of the adaptations necessary to transition from water to air.

**Keywords**:biofluids, Callinectes, Coenobita, terrestrialisation, mathematical model, advection diffusion

Olfaction, gathering information from dissolved chemical cues (odours), is a process important for animals in both marine and terrestrial habitats for mediating reproduction, finding food, and avoiding predators (e.g. [1, 2, 3, 4]). An important step in olfaction is odour capture, where many animals generate flow relative to their chemosensory organs. During odour capture, this fluid movement serves several purposes, including the transport of odourant molecules close to olfactory receptors at the surface of the organ and the acquisition of temporal and spatial information about the odour source (reviewed by [5, 6, 7]).

Many animals, including marine crustaceans and insects, use arrays of bristle-like chemosensory hairs in order to capture odours. In addition to olfaction, bristled arrays are common tools for a variety of tasks involving fluid-structure interactions, including feeding, swimming, and flying, in a regime where inertial and viscous forces are balanced [8]. At this scale, bristled arrays typically act as a solid surface, but there may be moments of higher velocity, interactions with surfaces, or increased spacing between bristles such that the arrays act as leaky rakes. Animals have creative ways of taking advantage of this transition. For example, copepods, small marine crustaceans, will slowly open their bristled feeding appendages to pull in water, and then quickly slap the appendages together to capture plankton between the bristles [9]. The smallest flying and swimming insects use bristled wings to reduce the force required to

clap wings together and fling them apart [10].

When animals transition from water to air during the process of terrestrialisation, the properties of the fluid change drastically: the density ($\rho$) of air is 1/1000 of water, dynamic viscosity ($\mu$) of air is 50 times less than water, and diffusion coefficient ($D$) of similar chemicals typically is thousands of times greater in air than in water. These changes will affect both fluid-flow patterns (advection) and molecular diffusivity (diffusion). Changing fluid will alter the antennules' Reynolds number ($Re = UL\rho/\mu$), a dimensionless number describing the ratio of inertial to viscous forces in fluid flow, indicating a major change in advective patterns surrounding the hairs. Additionally, the Péclet number ($Pe = UL/D$) is used to determine the relative importance of advection and diffusion in mass transport where $Pe << 1$ indicates diffusion-dominated transport and $Pe >> 1$ indicates advection-dominated transport. For antennules moving from water to air, values for $Pe$ cross this threshold from advection-dominated transport in water to diffusion-dominated transport in air.

Although it is clear that this transition from water to air alters the dynamics of odour capture, early terrestrialisation events that occurred deep in time (many hundreds of millions of years ago) leave few clues as to how odour capture in air evolved. Studying recent examples of terrestrialisation can provide insight into the general process of adapting odour capture to air.

One example of a relatively recent event is the split between marine and terrestrial hermit crabs (about 50 million years ago [11]). Marine and terrestrial hermit crabs capture odours with dense arrays of bristle-like chemosensory hairs, called aesthetascs, which they flick back and forth using antennules (Fig. 1). These arrays operate at the same scale where a bristled surface can act as either a solid surface or a leaky rake [7]. Previous work suggests that the aesthetasc arrays of marine crabs act as leaky rakes during the flick or downstroke. During

the return stroke, the arrays trap water between the hairs [12]. This sequence creates a flow-no flow pattern within the aesthetasc array, allowing marine crabs to take discrete samples of odour-containing water [7, 13, 14]. The ability to discretely sample is an important aspect of odour capture [15]. The flexibility of the marine crab's aesthetascs also helps to drive water into the array during the flick since hydrodynamic drag forces the hairs apart [12, 16] (Fig. 1). In contrast, the aesthetascs of terrestrial hermit crabs are short, stiff, and lay shingle-like close to the body of the antennule or flagellum (Fig. 1) [17]. The gaps between aesthetascs for terrestrial crabs are much smaller than those of the marine crabs. Terrestrial hermit crabs lack the flow-no flow pattern seen in marine-crab arrays [18].

These differences in hair-array morphology suggest that terrestrialisation has significant consequences for the physical process of odour capture. Although it is well understood that the physical demands organisms experience in air and water are strikingly different, very few studies have directly compared those demands in related species. This is due to the inherent limitations of traditional techniques for studying odour capture. The aesthetasc arrays of crabs are too small to observe fluid flow directly. Measuring and comparing performance through animal experiments in two fluid habitats on a single species is not possible due to various physiological and behavioural constraints. As a result, studies of odor capture are generally limited to quantifying the performance of a single species (e.g. [5, 19, 7]) or finding correlations between morphology and habitat (e.g. [20]).

We present a novel approach to studying odour capture in different fluid habitats using a computational model of odour capture. Previously, odour capture by aesthetascs has been simulated by coupling flow and diffusion near the hairs of a single species [13, 14, 21]. In each case, the flow fields were either taken from measurements on dynamically scaled models or from numerical simulations of a single fluid environment. In all cases, the numbers of hairs

were limited to arrays with either three aesthetascs [13, 14] or two aesthetascs [22].

In this paper, we model the advection and diffusion of a chemical gradient in air and water through the aesthetasc arrays of a terrestrial hermit crab (the ruggie hermit crab, *Coenobita rugosus*) and a marine crab (the blue crab, *Callinectes sapidus*), which closely resemble the arrays of marine hermit crabs. Due to the complex arrangement and large number of haphazardly arranged aesthetascs of the marine crab (on the order of hundreds), it is not feasible to compute unsteady flow fields in 2D or 3D. This is due to the fact that the full Navier-Stokes equations must be solved with sufficiently high resolution to capture both the advection and diffusion of a chemical gradient through a complex moving boundary (see the Materials and Methods and Supplemental Information for a more detailed explanation).

Given the challenges described above, we combine measured flow fields taken from dynamically scaled, physical models with numerical simulations of the advection, diffusion, and uptake of chemical gradients. By coupling flow fields with diffusion and uptake, we have created a standardised odour-capture metric to directly compare the performance of each species in terrestrial and aquatic environments. Quantifying the performance of each species' hair array in both habitats reveals the role of morphology during the process of terrestrialisation. Since theoretical models give us control over each aspect of odour transport (e.g. advection, diffusion, and the role of morphology), we can quantify the effect of each of these parameters independently.

## Materials and Methods

Ideally, we would be able to model and numerically simulate the full Navier-Stokes equations with an moving array and the advection and diffusion of a chemical gradient in three dimensions. Currently, it is not feasible to solve for the three-dimensional fluid flow through about 200 hairs at intermediate Reynolds numbers where insufficient resolution can dramatically alter

the flow near the hairs. Given the intermediate Reynolds number regime ($0.1 < Re < 10$), it is also necessary to solve the full Navier-Stokes equations, and the Stokes or Oseen's approximations are not appropriate. To accurately compute the flow through structures in this sensitive Reynolds number regime, extremely small computational grids are needed. Assuming, 20 grid points is sufficient in one dimension to accurately resolve the flow between each pair of aesthetascs, approximately 100,000,000 grid points would be needed to resolve the flow in a 2 mm by 2 mm by 2 mm cube, based on the spacing of the marine crabs hairs shown in Fig. 2. This resolution is prohibitive, even with today's advanced computational capabilities. We present our mixed model, based broadly on Stacey et al. 2002 [13], as a solution to this challenge.

## Particle Image Velocimetry (PIV)

Velocity fields used in the mathematical model and numerical simulations were measured on dynamically scaled physical models of the antennules of the terrestrial hermit crab, *Coenobita rugosus* Milne-Edwards 1836 (representing the terrestrial-crab morphology), and of the blue crab, *Callinectes sapidus* Rathburn 1896 (representing the marine-crab morphology). These PIV fields are from previously published studies (marine crab: [12], terrestrial crab: [18]). Details of the physical models, the PIV setup, and PIV post-processing can be found therein. Fig. 2 contains a brief summary of these methods, and more details can also be found in the Supplementary Information (SI) to this paper.

We simulated flow through the arrays of both species in different fluids using geometrically scaled physical models of the flagellum and aesthetasc array. The models were moved at velocities, ($U$), required to match the Reynolds numbers of each fluid ($Re = UL/\nu$) based on the aesthetasc diameter ($L$) and the fluid's kinematic viscosity ($\nu = \mu/\rho$). Fluid velocities were measured using particle image velocimetry (Fig. 2 for marine crabs and Fig. 3 for terrestrial

crabs). Data were taken within a laser sheet that bisected a section of the flagellum and aesthetasc array. This created a cross section of each aesthetasc, as shown by the white circular or elliptical shapes immersed in the velocity fields. Note that in the case of the terrestrial crab, there were about 12 ellipse-shaped hairs. For the marine crab there were about 151 circular hairs. Velocity fields are scaled to the characteristic velocity of the animal during flicking.

## Mathematical Modelling

We have developed a mathematical model to couple the experimental velocity data (collected via PIV as described above) with the advection, diffusion, and uptake of the odour concentration. We have solved

$$\frac{\partial C}{\partial t} + \frac{\partial (uC)}{\partial x} + \frac{\partial (vC)}{\partial y} = D\left(\frac{\partial^2 C}{\partial x^2} + \frac{\partial^2 C}{\partial y^2}\right), \tag{1}$$

for the odour concentration, $C(x, y, t)$ in a given domain $\Omega$, with the steady-state experimental velocity fields, $(u, v)$ and diffusion coefficient, $D$. The details of the numerical method and pre-processing of the experimental velocity fields are in the Supplemental Information to this paper.

We have measured the odour capture of each crab by placing aesthetascs in $\Omega$ (as located in the collection of the PIV data) and observing how much odour was captured by each aesthetasc and removing that odour from the environment as it was captured. Beyond varying the environmental conditions, we have considered two initial conditions for the model, a thin and a thick filament. We have developed a numerical method to solve this mathematical model for the odour concentration captured. The odour concentration presented in Fig. 4 is standardised as described below to allow for comparisons between different simulation cases. Further details of the model and on the numerical method are given in the SI.

To determine how the altered flow patterns would impact odour capture, we simulated

chemical transport to the aesthetasc using a model of advection, diffusion, and uptake. The velocity fields were obtained from the previously described experimental measurements. A no-slip boundary condition was enforced at the boundary of each aesthetasc. The diffusion coefficients, ($D_{air},\ D_{water}$), were chosen to reflect the diffusivity of common odourants in air or water. The initial condition of the chemical gradients was chosen to model the natural conditions of odourants. These choices included 'thin' filaments for water (a narrow filament that extends the vertical distance of the domain) and 'thick' filaments for air (a filament that extends beyond the domain in the horizontal axis) (see Supplemental Information for details).

For each time step, odourant that diffuses into the aesthetasc is recorded and removed. Total concentrations captured were standardised by the maximum initial concentration of the filament and the total circumference of the aesthetascs. Each set of conditions was repeated using three unique sets of experimental velocity fields that represented independent replicates of the arrays used in antennule flicking.

With this model, we were able to simulate the environmental conditions reflective of either air or water in two parts: 1) using a diffusion coefficient of a typical molecule in either air ($D_{air}$) or water ($D_{water}$), and 2) using experimental velocity fields for the downstrokes and return strokes for antennules flicking observed at Reynolds number in air ($Re_{air}$) or water ($Re_{water}$). Values of the Reynolds numbers used can be found in Tables 1 (for *Callinectes sapidus*) and 2 (for *Coenobita rugosus*) in the SI. We were also able to pair non-matching environmental conditions (e.g. diffusion of air ($D_{air}$) with the velocity fields of water ($Re_{water}$)) to investigate the effect of each on odour capture.

For each marine crab simulation, the downstroke velocity field is applied for 0.0152 s, then the return stroke velocity field is applied for 0.0248s, and then the velocity is set to 0 for a rest period of 0.24 s. For the terrestrial crab simulations, the downstroke velocity field is applied

for 0.0782 s and the return stroke velocity field is applied for 0.0603 s. The diffusion coefficient, $D$, depends on whether the crabs are in water or in air. Values are given in Tables 1 and 2.

In order to make the simulations directly comparable between fluids and morphologies, results were standardised in two ways. First, we divided the raw concentration captured by the maximum concentration of the initial condition for each simulation ($C_\infty$), to find the fraction of chemical captured ($C/C_\infty$). Second, we divided the fraction of chemical captured by an effective capture area of each array, $d$, described below. When both standardisations are performed, the adjusted captured concentration is reported as $C/(C_\infty \cdot d)$.

Since each species' array had different areas of contact with odour-containing fluid, we standardised this surface by defining an effective capture area of the array as sum of the diameters of all aesthetascs that captured an unadjusted concentration of at least $1 \times 10^{-10}$. For the terrestrial crabs, every hair caught at least this much concentration for every case, so the effective capture area was the sum of the diameters of all aesthetascs. For marine crabs, simulations yielded different effective captures areas as some aesthetascs in each simulation captured no chemical (Fig. 4). The number of hairs capturing a minimum concentration was multiplied by the aesthetascs' circumference to find the effective capture area.

## Statistical Analysis

Values of the amount of chemical captured are the result of three replicate runs ($n = 3$) using three replicate sets of PIV flow fields (downstroke and return stroke data). In Fig. 5, all values are reported with 95% confidence intervals. For comparisons with non-overlapping confidence intervals, we assumed that the comparisons were significant at $\alpha = 0.05$ level. For comparisons with overlapping confidence intervals, we tested each using a double-tailed Welch's t-test with a Bonferroni correction. The t-statistic and adjusted $p$ values are reported with each of these

comparisons and treated as significant at $\alpha = 0.05$. All statistical analyses were completed in R using the basic statistics package [23].

# Results

## Changing fluids alters flow patterns for marine but not terrestrial crabs

For the marine crab in water, fluid flow within the array demonstrates the classic flow-no flow pattern of marine malacostracan sniffing reported elsewhere [7, 12, 16, 19]. Flow is relatively high during the downstroke and near zero during the return stroke. This can be seen by comparing the velocity magnitudes within the array in the bottom left and bottom right panels in Fig. 2. This pattern is highly dependent on the Reynolds number and the spacings between aesthetascs. Previous studies have found that decreasing the Reynolds number of the downstroke below approximately 0.6 dramatically reduces flow within the array [7, 12].

During terrestrialisation, the fluid in which the aesthetasc array is immersed changes from water to air. Although our models of the downstroke of a marine crab in air are set to the same speed as in water, the Reynolds number decreases by a factor of 16 due to the fact that the kinematic viscosity of air is higher than water. As a result, the downstroke Reynolds number drops below the value that allows flow within the array, and the flow-no flow pattern disappears. Air flow within the array during both the downstroke and return stroke are near zero (top two panels of Fig. 2).

For the terrestrial crab, flow within the array indicates the absence of the flow-no flow pattern in air [18]. Flow within the aesthetasc array remains low for both the downstroke and return stroke (top two panels of Fig. 3). Remarkably, fluid flow within the array is also near-zero for terrestrial crabs flicking in water (bottom two panels of Fig. 3), despite the fact

that the Reynolds number increases by an order of magnitude. In summary, the configuration of the terrestrial crab array does not allow significant flow within the array for either stroke or fluid medium, suggesting that diffusion dominates over advection for odour capture.

## Simulating odour capture reveals antennule specialisation

To compare the performance of the crabs in both environments and with both initial conditions, eight simulations were performed for each species. In Fig. 5, panels A and B show the results for a thin filament, and panels C and D show the results for a thick filament. The simulations performed using $D_{air}$ are shown in red, and those performed with $D_{water}$ are shown in blue. All solid lines represent simulations that use the morphology of the marine-crab array, and the dashed lines show results for the terrestrial-crab array. Panels A, C, and D use the $Re$ appropriate to the fluid medium ($Re_{air}$ is shown in red and $Re_{water}$ is shown in blue) except for panel B where the $Re$ are swapped. In this panel, $D_{air}$ and $Re_{water}$ are shown in red, and $D_{water}$ and $Re_{air}$ are shown in blue. Finally, the flick durations ($T$) are species specific in panels A, B, and C and are swapped for D.

Each crab captures a greater fraction of available odourant in their native fluid environments. In air, terrestrial crabs ($Re_{air}$, $D_{air}$) capture 2.0 times more odourant than marine crabs ($Re_{air}, D_{air}$) when presented with a thin filament and 2.9 times more when presented with a thick filament (Figs. 5A and 5C, red lines). In water, marine crabs ($Re_{water}$, $D_{water}$) capture 6.8 times more concentration than terrestrial crabs ($Re_{water}$, $D_{water}$) for a thin filament and 17 times more for a thick filament (Figs. 5A and 5C, blue lines). Further, the flow-no flow pattern is highly beneficial for marine crabs. The benefit of water flow within the array is so great that the performance of marine crabs in air and water is comparable when the capture area is controlled despite several orders of magnitude difference in diffusivity (Fig. 5A, solid

lines).

If the diffusivity of air ($D_{air}$) is used, marine crab arrays with greater fluid penetration ($Re_{water}$) capture more odourant than simulations with limited fluid penetration in the array ($Re_{air}$) (Figs. 5A and 5B, solid red lines). When diffusivity of water ($D_{water}$) is used, marine crabs in flows with less fluid penetration during the downstroke ($Re_{air}$) capture less odour than in simulations with more fluid penetration ($Re_{water}$) (Figs. 5A and 5B, solid blue lines). Note that this difference is not, however, significant ($t = 3.4$, adjusted $p = 0.33$).

The transition to Reynolds number of air affects the distribution of odour capture in the marine crab's array. In water, fluid penetration into the marine crab array results in a large number of aesthetascs participating in odour capture at a greater depth in the array (Fig. 4A). When moved to air, fewer aesthetascs capture odours, and these aesthetascs are restricted to the very edge of the array (Fig. 4C).

In contrast, odour capture for terrestrial crabs in air does not depend upon changes in flow within the array. For both air and water, odour capture is restricted to the outer edges of its array (Figs. 4B and 4D). When the diffusion coefficient is controlled, total odour capture rates are also not significantly different for flicking with the Reynolds numbers of air or water (for $D_{air}$: Figs. 5A and 5B, dashed red lines; $t = 0.95$, adjusted $p = 1$; for $D_{water}$: Figs. 5A and 5B, dashed blue lines; $t = -0.99$, adjusted $p = 1$).

The same morphology that gives terrestrial crabs an advantage in air negatively impacts the odour-capture performance in water due to the change in diffusivity and the lack of a flow-no flow pattern. Since the diffusion coefficient is smaller in water and no water penetrates the array to bring odour molecules close to the aesthetascs, odour capture from thin filaments in water is only a small fraction of that captured in air (Fig. 5A, blue and red dashed lines). The reduction of odour capture in water is also found for thick filaments (Fig. 5C, dashed blue and

red lines).

The differences in fluid flow and diffusion coefficients are not the only features of the animals' environment which change between water and air. High-concentration odour filaments, created by turbulent mixing of fluid, differ in many ways between air and water. One feature is the size of these filaments; odour filaments in air are much wider than those of water. Consideration of this feature further enhances the fluid-specific benefits of each aesthetasc-array morphology. When flicking through a thick filament, terrestrial crabs capture 123 times more odourant in air than they do in water (Fig. 5C, dashed red and blue lines). The difference in performance between air and water for a thin filament is smaller than the difference in performance for a thick filament, being only about one order of magnitude (Fig. 5A, dashed red and blue lines).

When comparing Figs. 5C and 5D, the duration of the flick ($T$) was altered from the biologically relevant case (long flick for terrestrial crabs, short flick for marine crabs) to the swapped case (long flick for marine crabs, short flick for terrestrial crabs). The terrestrial crab's longer duration of flicking seems to account for the increased odour capture in thick filaments using the properties of both air and water. Increasing the duration of the marine crab's flick to match that of a terrestrial crab's flick eliminates the performance difference between the two morphologies, as can be shown by comparing each species in Figs. 5C and 5D. Marine crabs have a slight advantage in air over terrestrial crabs ($D_{air}$ and $Re_{air}$) when the flick duration is increased (increase of 60%) that is significant (Fig 5C, dashed red line and Fig 5D, solid red line; $t = -7.74$, adjusted $p = 0.04$).

# Discussion

Both fluid-flow patterns and diffusion impact the ability of decapod antennules to capture odours from surrounding fluid. For these simulations, both marine and terrestrial crabs have

$Pe \approx 1000$ in water and $Pe \approx 0.1$ in air (see Tables 1 and 2 for Péclet number calculations). These indicate that each species, in addition to experiencing very different flows within their aesthetasc arrays, naturally inhabits a drastically different transport regime than the other.

Terrestrial hermit crabs have reduced aesthetasc-array features and, as a result, lack the flow-no flow pattern demonstrated by marine crabs in water. These changes confer a performance benefit in transport regimes in which diffusion is dominant ($Pe < 1$). However, when operating in a transport regime where advection is important ($Pe > 1$) as in water, loss of the flow-no flow pattern has rendered terrestrial hermit crabs all but nonfunctional in water when compared to marine crabs. The flow patterning exhibited by marine crabs is so effective in water that it rivals the amount of odourant capture by terrestrial crabs in air, despite the diffusion coefficient of water being several orders of magnitude less than that of air.

Our results also suggest that there are heavy selective pressures that constrain the morphology and kinematics of the antennules of malacostracan crustaceans in water. Terrestrialisation of coenobitid crabs (terrestrial hermit crabs in the genus *Coenobita* and the robber crab, *Birgus latro*) results in the loss of the flow-no flow pattern. This adaptation allows for superior odour-capture performance in air as compared to marine crabs but would result in a devastating drop in performance in water. Since the terrestrial crab's antennules exist in a diffusion-dominated transport regime and flow-no flow pattern is no longer necessary in air, the antennules may be reduced without a loss in performance. The longer duration flick in air is also advantageous, and we see that terrestrial crabs do, in fact, flick for longer times [24]. These differences are further augmented when the initial conditions of the odourant are reflective of odour distributions in air (e.g. thick filaments).

The life history of terrestrial hermit crabs also reflect these differences in performance. Hermit crab larvae initially live in the water column where they are dispersed by currents. At

this stage, their antennule morphology mimics marine species [25, 26]. As they develop, they settle near land and undergo metamorphosis [25, 27]. During post-settlement metamorphosis, the juveniles emerge from the sea to live permanently on land and exhibit the adult antennule morphology [27, 28, 26].

Additional pressures, such as evaporation, may also play a role in the morphology of the terrestrial hermit crab array. Ghiradella et al. [17] suggested that a reduction in the area of permeable cuticle in the aesthetasc array may limit water loss. The area of permeable cuticle would be lowered in the case of the shortened aesthetascs of the terrestrial hermit crab, giving an advantage to this reduced morphology in air. Their conjecture was further supported by other studies of coenobitid crabs [29, 30]. Evaporative water loss in air may select for reduced arrays, while the need for a flow-no flow pattern in water may drive arrays towards a lengthened morphology.

These results have implications for other terrestrialisation events in decapod crustaceans, the group which includes lobsters, crayfish, crabs, and shrimp. For example, terrestrial species within the Brachyura (an infraorder of 'true' crabs that does not include hermit crabs) also exhibit changes in antennule morphology. The changes to antennules within the Brachyura are consistent with the reduced pressures of sniffing in water and include reduced aesthetasc length and number, lack of flicking, and reduced brain area dedicated to aesthetasc-mediated olfaction [31]. It is unclear why the hermit crabs, a lineage of anomuran crabs, successfully adapted antennules for olfaction in air while no lineages within the Brachyura have done so. Similarly, most other terrestrialised lineages in the Malacostraca (the largest class of crustaceans) [32, 33] have not adapted antennules for olfaction in air.

Zooming out from malacostracans, the transition of hexapods (the group containing insects) to land was followed by one of the largest radiations in the history of life. Chemosensory sen-

348 silla on the second antennae of insects exhibit significant morphological diversity for capturing
349 odours in air [34], and many features common to insect sensilla are also found convergently in
350 coenobitids, such as housing basal bodies and cilia within a lymph space inside the flagellum
351 and similar electroantennographic responses to airborne odours [29]. It is possible that the
352 transition from a low Péclet number system, dominated by diffusive transport, removed the
353 constraints associated with high Péclet number systems such as those associated with discrete
354 odour sampling in marine crabs. This shift in the relative importance of advection and diffusion
355 potentially allowed diverse sensory morphologies to develop in insects.

356 In addition to evolutionary insights, our results suggest that the open, hair-like design of
357 crabs' chemosensory arrays are an effective strategy for chemical sensing in both water and air
358 without the constraints of drawing fluid through an enclosed space such as mammalian sinuses.
359 The hair-like aesthetascs of marine crabs capture a large fraction of odourant in air and water,
360 but the performance of the array was highly sensitive to the arrangement, size, and shape of
361 the aesthetascs within its array as well as the kinematics with which the array was moved. Here
362 we have shown that both sensitivity of the chemosensory structure and the kinematics of the
363 array must be considered to create an effective biomimetic sensor.

## 364 Acknowledgments

365 This work was supported by a NSF Research and Training Grant DMS #0943851 (to R. McLaugh-
366 lin, R. Camassa, L. Miller, G. Forest, and P. Mucha), an NSF CAREER Award DMS #1151478
367 (to L. Miller), and NSF PoLS #1504777 (to L. Miller) and #1505061 (to S. Khatri). Special
368 thanks to: Steven Piantadosi for comments on the manuscript; Karin Leiderman and Mimi
369 Koehl for support on this project.

# References


[1] Hazlett, B., 1969 Individual recognition and agonistic behaviour in *Pagurus bernhardus*. *Nature* **222**, 268–269.

[2] Gleeson, R., 1980 Pheromone communication in the reproductive behavior of the blue crab, *Callinectes sapidus*. *Marine Behavior and Physiology* **7**, 119–134.

[3] Gherardi, F., Tricarico, E. & Atema, J., 2005 Unraveling the nature of individual recognition by odor in hermit crabs. *Journal of Chemical Ecology* **31**, 2877–2796.

[4] Gherardi, F. & Tricarico, E., 2007 Can hermit crabs recognize social partners by odors? and why? *Marine and Freshwater Behavioral Physiology* **40**, 201–212.

[5] Schmidt, B. & Ache, B., 1979 Olfaction: responses of a decapod crustacean are enhanced by flicking. *Science* **205**, 204–206.

[6] Moore, P. & Crimaldi, J., 2004 Odor landscapes and animal behavior: tracking odor plumes in different physical worlds. *Journal of Marine Systems* **49**, 55–64.

[7] Koehl, M., 2011 *Chemical Communication in Crustaceans*, chapter Hydrodynamics of sniffing by crustaceans, pp. 85–102. New York: Springer Verlag.

[8] Cheer, A. Y. L. & Koehl, M. A. R., 1987 Paddles and rakes: Fluid flow through bristled appendages of small organisms. *J. Theor. Biol.* **129**, 17–39.

[9] Koehl, M. A. R., 2004 Biomechanics of microscopic appendages: Functional shifts caused by changes in speed. *J. Biomech.* **37**, 789–795.

[10] Santhanakrishnan, A., Robinson, A. K., Jones, S., Lowe, A., Gadi, S., Hedrick, T. L. & Miller, L. A., 2014 Clap and fling mechanism with interacting porous wings in tiny insect flight. *J. Exp. Biol.* Doi: 10.1242/jeb.084897.

[11] Bracken-Grissom, H., Cannon, M., Cabezas, P., Feldmann, R., Schweitzer, C., Ahyong, S., Felder, D., Lemaitre, R. & Crandall, K., 2013 A comprehensive and integrative reconstruction of evolutionary history for Anomura (Crustacea: Decapoda). *BMC Evolutionary Biology* **13**, 1–28.

[12] Waldrop, L., Reidenbach, M. & Koehl, M., 2015 Flexibility of crab chemosensory sensilla enables flicking antennules to sniff. *Biological Bulletin* **229**, 185–198.

[13] Stacey, M., Mead, K. & Koehl, M., 2002 Molecule capture by olfactory antennules: Mantis shrimp. *Journal of Mathematical Biology* **44**, 1–30.

[14] Schuech, R., Stacey, M., Barad, M. & Koehl, M., 2012 Numerical simulations of odorant detection by biologically inspired sensor arrays. *Bioinspiration and Biomimetics* **7**, 016001.

[15] Schoenfeld, T., 2006 Special issue: What's in a sniff?: The contributions of odorant sampling to olfaction. *Chemical Senses* **31**, 91–92.

[16] Waldrop, L., Hann, M., Henry, A., Kim, A., Punjabi, A. & Koehl, M., 2015 Ontogenetic changes in the olfactory antennules of the shore crab, *Hemigrapsus oregonensis*, maintain sniffing function during growth. *Journal of the Royal Society Interface* **12**, 20141077.

[17] Ghiradella, F., Case, J. & Cronshaw, J., 1968 Structure of aesthetascs in selected marine and terrestrial decapods - chemoreceptor morphology and environment. *American Zoologist* **8**, 603–621.

[18] Waldrop, L. & Koehl, M., 2016 Do terrestrial hermit crabs sniff? air flow and odorant capture by flicking antennules. *J Royal Soc Interface* **13**, DOI: 10.1098/rsif.2015.0850.

[19] Reidenbach, M., George, N. & Koehl, M., 2008 Antennule morphology and flicking kinematics facilitate odour sampling by the spiny lobster, *Panulirus argus*. *Journal of Experimental Biology* **211**, 2849–2858.

[20] Mead, K., 2008 Do antennule and aesthetasc structure in the crayfish *Orconectes virilis* correlate with flow habitat? *Integr. Comp. Biol* **48**, 823–833.

[21] Nelson, J. M., Mellon, D. & Reidenbach, M. A., 2013 Effects of antennule morphology and flicking kinematics on flow and odor sampling by the freshwater crayfish, procambarus clarkii. *Chemical senses* **38**, 729–741.

[22] Pravin, S., Mellon, D. & Reidenbach, M., 2012 Micro-scale fluid and odorant transport to antennules of the crayfish, *Procambarus clarkii*. *J. Comp. Physiol. A* **198**, 669–681.

[23] Team, R. D. C., 2011 *R: A Language and Environment for Statistical Computing*. R Foundation for Statistical Computing, Vienna, Austria, http://www.r-project.org/ edition.

[24] Waldrop, L., Bantay, R. & Nguyen, Q., 2014 Scaling of olfactory antennae of the terrestrial hermit crabs *Coenobita rugosus* and *Coenobita perlatus* during ontogeny. *PeerJ* **in press**.

[25] Renae Brodie, A. W. H., 2001 Larval development of the land hermit crab coenobita compressus h. milne edwards reared in the laboratory. *Journal of Crustacean Biology* **21**, 715–732. ISSN 02780372, 1937240X.

[26] Harvey, A., Boyko, C., McLaughlin, P. & Martin, J., 2014 *Atlas of Crustacean Larvae*, chapter Infraorder Anomura, pp. 283–294. Johns Hopkins University Press.

[27] Brodie, R., 2002 Timing of the water-to-land transition and metamorphosis in the land hermit crab *Coenobita compressus* H. Milne Edwards: evidence that settlement and metamorphosis are decoupled. *Journal of Experimental Marine Biology and Ecology* **272**, 1–11.

[28] Waldrop, L., 2013 Ontogenetic scaling of the olfactory antennae and flicking behavior of the shore crab, *Hemigrapsus oregonensis*. *Chemical Senses* **38**, 541–550.

[29] Stensmyr, M., Erland, S., Hallberg, E., Wallen, R., Greenaway, P. & Hansson, B., 2005 Insect- like olfactory adaptations in the terrestrial giant robber crab. *Current Biology* **15**, 116–121.

[30] Tuchina, O., Koczan, S., Harzsch, S., Rybak, J., Wolff, G., Strausfeld, N. J. & Hansson, B. S., 2015 Central projections of antennular chemosensory and mechanosensory afferents in the brain of the terrestrial hermit crab (coenobita clypeatus; coenobitidae, anomura). *Frontiers in Neuroanatomy* **9**. ISSN 1662-5129. (doi:10.3389/fnana.2015.00094).

[31] Krieger, J., Braun, P., Rivera, N., Schubart, C., Müller, C. & Harzsch, S., 2015 Comparative analyses of olfactory systems in terrestrial crabs (Brachyura): evidence for aerial olfaction? *PeerJ* **3**, e1433.

[32] Bliss, D. & Mantel, L., 1968 Adaptations of crustaceans to land - a summary and analysis of new findings. *American Zoologist* **8**, 673.

[33] Greenaway, P., 2003 Terrestrial adaptations in the Anomura (Crustacea: Decapoda). *Memoirs of Museum Victoria* **60**, 13–26.

[34] Keil, T., 1999 Morphology and development of the peripheral olfactory organs. In *Insect Olfaction* (ed. B. Hansson), chapter 1, pp. 5–47. Springer Verlag.

[35] Legall, N. & Poupin, J., 2016. CRUSTA: Database of Crustacea (Decapoda and Stomatopoda), with special interest for those collected in French overseas territories. Available at: http://crustiesfroverseas.free.fr/.

[36] NOAA, 2016. National Oceanic and Atmospheric Administration Fisheries Image Gallery. Available at: http://www.nmfs.noaa.gov/gallery/images/.

[37] Sveen, J., 2004 *An introduction to MatPIV v. 1.6.1: Mechanics and Applied Mathematics.* Dept. of Mathematics, Univ. of Oslo, Oslo, 2nd edition.

Table 1: Values used for creating velocity fields using dynamically scaled physical models of the terrestrial hermit crab, *Coenobita rugosus*. *Using $Re = UL/\nu$, aesthetasc diameter $L = 1.5 \times 10^{-5}$m [24]. † Using $Pe = UL/D$, aesthetasc diameter $L = 1.5 \times 10^{-5}$m [24]

| Parameter | Air | Water |
|---|---|---|
| Diffusion coefficient, $D$ ($m^2s^{-1}$) | $6.02 \times 10^{-6}$ | $7.84 \times 10^{-10}$ |
| Kinematic viscosity, $\nu$ ($m^2s^{-1}$) | $8.50 \times 10^{-6}$ | $1.05 \times 10^{-6}$ |
| Downstroke speed, $U$ (m $s^{-1}$) | 0.063 | 0.063 |
| Actual Downstroke $Re^*$ | 0.11 | 0.90 |
| Modelled Downstroke $Re^*$ | 0.098 | 0.77 |
| Downstroke $Pe^\dagger$ | 0.16 | 1,200 |
| Return stroke speed, $U$ (m $s^{-1}$) | 0.11 | 0.11 |
| Actual Return stroke $Re^*$ | 0.19 | 1.6 |
| Modelled Return stroke $Re^*$ | 0.21 | 0.77 |
| Return stroke $Pe^\dagger$ | 0.27 | 2,100 |

Table 2: Values used for creating velocity fields using dynamically scaled physical models of the marine blue crab, *Callinectes sapidus*. *Using $Re = UL/\nu$, aesthetasc diameter $L = 9.0 \times 10^{-6}$m [12]. †Using $Pe = UL/D$, aesthetasc diameter $L = 9.0 \times 10^{-6}$m [12]

| Parameter | Air | Water |
|---|---|---|
| Diffusion coefficient, $D$ ($m^2s^{-1}$) | $6.02 \times 10^{-6}$ | $7.84 \times 10^{-10}$ |
| Kinematic viscosity, $\nu$ ($m^2s^{-1}$) | $8.50 \times 10^{-6}$ | $1.05 \times 10^{-6}$ |
| Downstroke speed, $U$ (m $s^{-1}$) | 0.17 | 0.17 |
| Actual Downstroke $Re^*$ | 0.18 | 1.5 |
| Modelled Downstroke $Re^*$ | 0.20 | 1.6 |
| Downstroke $Pe^\dagger$ | 0.25 | 2,000 |
| Return stroke speed, $U$ (m $s^{-1}$) | 0.061 | 0.061 |
| Actual Return stroke $Re^*$ | 0.060 | 0.52 |
| Modelled Return stroke $Re^*$ | 0.070 | 0.57 |
| Return stroke $Pe^\dagger$ | 0.091 | 700 |

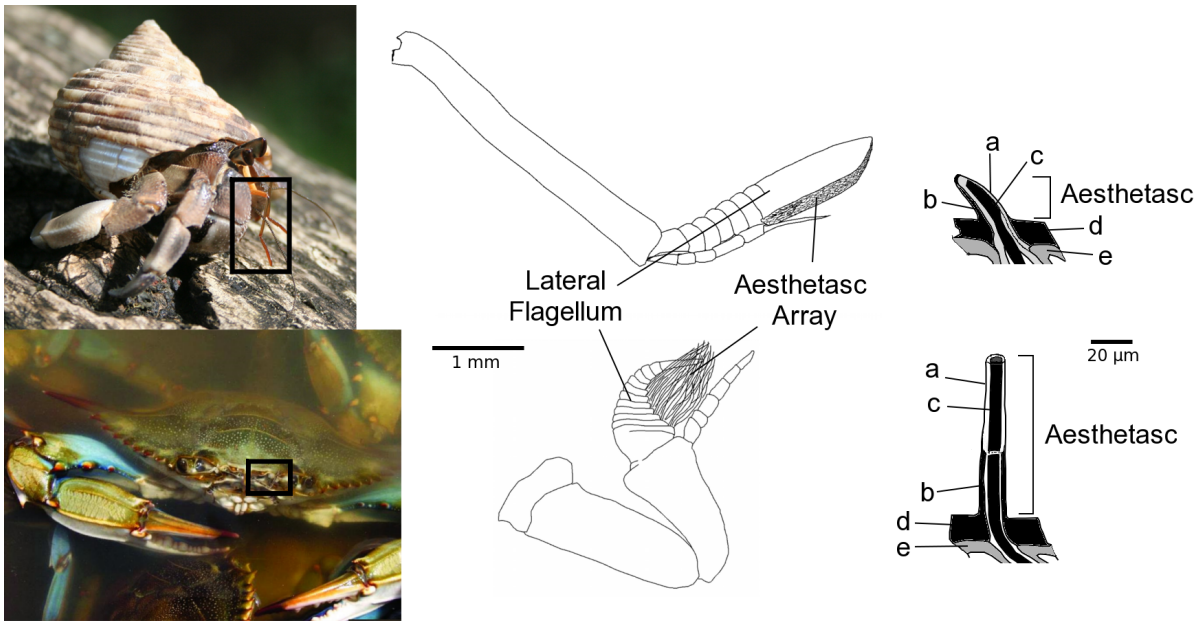


Figure 1: Top left: adult terrestrial hermit crab *Coenobita rugosus* with black box around antennule, photo credit: J. Poupin, Moorea Island, photo in [35]. Bottom left: adult marine crab *Callinectes sapidus* with black box around antennule, photo credit: NOAA Fisheries Image Gallery [36]. Middle: Schematic diagrams of the antennules of the terrestrial hermit crab (top) and the marine crab (bottom). Right: schematic diagram of individual aesthetascs of terrestrial hermit crab (top) and marine crab (bottom) after Fig. 29 in [17]; a - area of thinned cuticle able to accept odourants, b - area of thickened, impenetrable cuticle around the aesthetasc, c - dendrite branches, d - cuticle, e - sheaths.

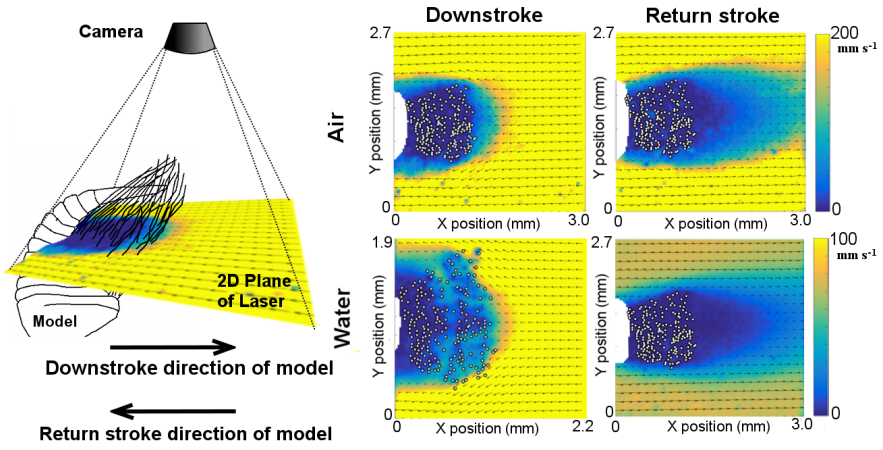


Figure 2: Diagram of particle image velocimetry (PIV) setup and results for the marine crab dynamically scaled physical model. Left: The model was dragged through a tank of oil with reflective marker particles in the direction indicated by the arrows. The camera was mounted above the model antennule and captured images at 60 fps. Particle movements were illuminated in a 2D plane created by the laser. Velocities were reconstructed from consecutive image pairs using MatPIV v1.6.1 [37] (for more details, see SI and [12, 18]). Right: PIV results. Top left - downstroke in air; top right - return stroke in air; bottom left - downstroke in water; bottom right - return stroke in water. Aesthetascs are white outlined in black, the flagellum of model is shown in white and lies to the left of each vector field.

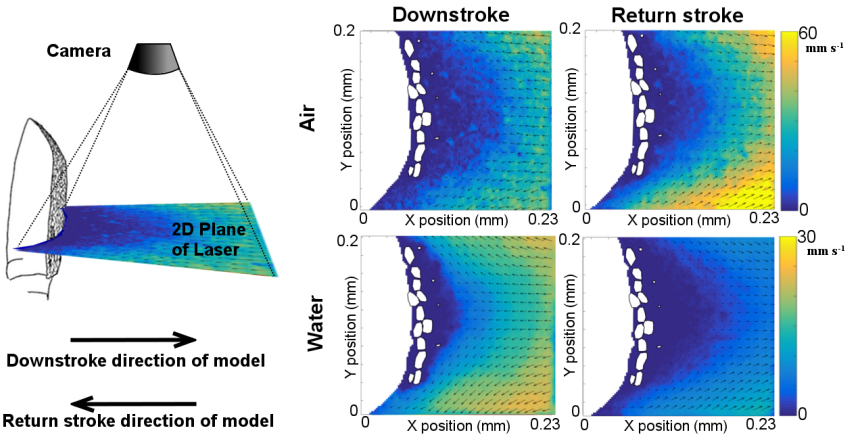


Figure 3: Diagram of PIV setup for the dynamically scaled physical model of the terrestrial hermit crab antennule. Left: the camera mounted above the model antennule shows the capture area of the 2D plane created by the laser where velocity vector fields were measured. Right: PIV results. Top left - downstroke in air; top right - return stroke in air; bottom left - downstroke in water; bottom right - return stroke in water.

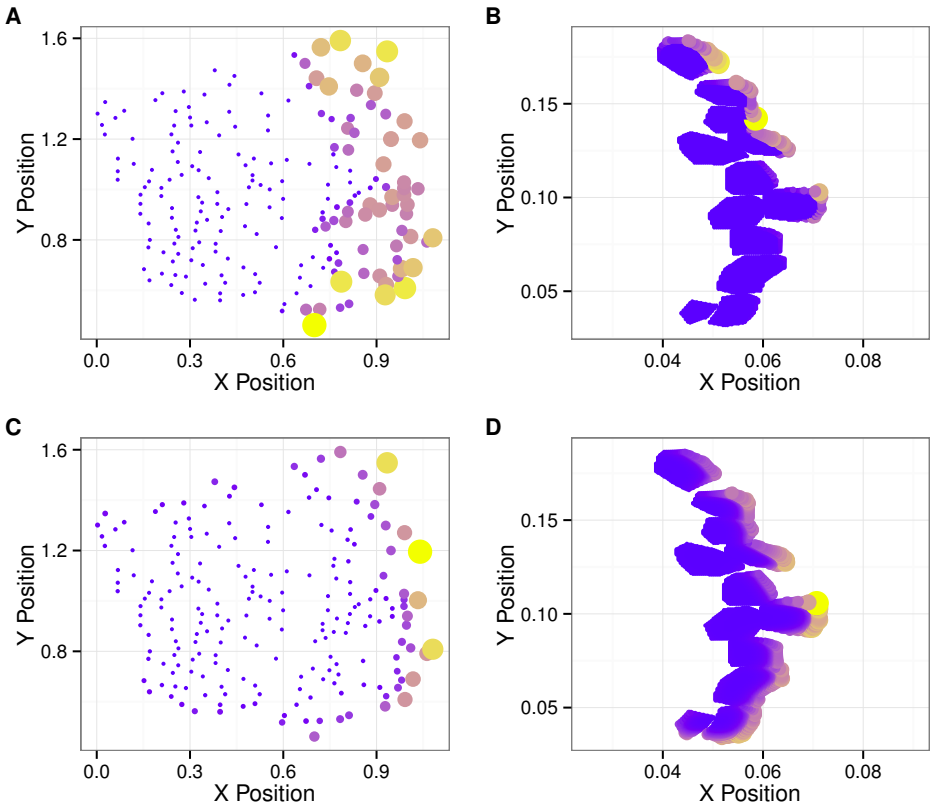


Figure 4: Normalised odor concentration absorbed by individual aesthetascs where size and color correspond to total amount for the marine-crab array (left) and terrestrial-crab array (right) in a thin odour filament. A,B: flicking in water ($Re_{water}, D_{water}$); C,D: flicking in air ($Re_{air}, D_{air}$). Yellow represents high odour concentrations and blue represents low concentrations.

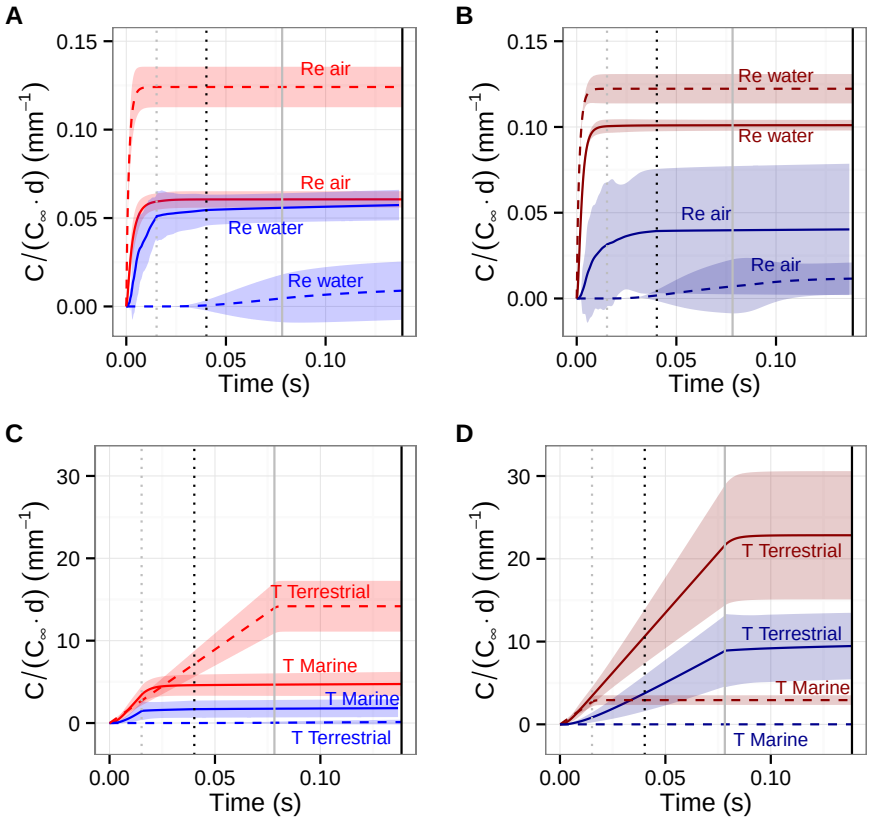


Figure 5: Total capture of available odour concentration ($C/(C_\infty \cdot d)$ in $\text{mm}^{-1}$) reported with 95% confidence intervals versus simulation time (in s) by aesthetascs flicking through thin (A,B) and thick (C,D) odour filaments. A: For marine crabs (solid lines) and terrestrial crabs (dashed lines) in air ($Re_{air}$, $D_{air}$; red lines) and water ($Re_{water}$, $D_{water}$; blue lines). B: For marine crabs (solid lines) and hermit crabs (dashed lines) with altered Reynolds numbers: $Re_{water}$, $D_{air}$ (dark red) and $Re_{air}$, $D_{water}$ (dark blue). C: For marine crabs (solid lines) and terrestrial crabs (dashed lines) in air ($Re_{air}$, $D_{air}$; red lines) and water ($Re_{water}$, $D_{water}$; blue lines). (continued on next page)

Figure 5: (continued) D: For marine crabs (solid lines) and terrestrial crabs (dashed lines) in air ($Re_{air}$, $D_{air}$; dark red) and water ($Re_{water}$, $D_{water}$; dark blue) with reversed flick durations ($T$): terrestrial-crab morphology flicks with duration of marine crab and marine-crab morphology flicks with duration of terrestrial crab. In all plots, grey, dotted, vertical line gives duration of marine crab downstroke and black, dotted, vertical line gives duration of marine crab flicking. Grey, solid, vertical line gives duration of terrestrial crab downstroke and black, solid, vertical line gives duration of terrestrial crab flicking. Movies of simulations can be found in the SI.